JNPS 10 (2): 110 – 120 (2024)
ISSN: 2392-473X (Print), 2738-9537 (Online)

Research Article ©Nepal Physical Society
doi.org/10.3126/jnphyssoc.v10i2.79498

Numerical Solution of Parabolic Partial Differential Equation by Using Finite Element Method

Nishan Upreti,[1] Jeevan Kafle,[1,*)] Chet Nath Tiwari,[2] and Hari Prapanna Kandel[3]

[1)]*Central Department of Mathematics, Tribhuvan University, Kirtipur, Kathmandu, Nepal*
[2)]*Tri-Chandra Multiple Campus, Tribhuvan University, Kathmandu, Nepal*
[3)]*Golden Gate International College, Buttisputali, Kathmandu, Nepal*

Abstract. Partial differential equations (PDEs) are used in the real world to model physical phenomena such as heat, wave, Laplace, and Poisson equations. For regular shape domains, the heat equation can be solved analytically; however, for irregular domains, the computation of the solution is difficult and numerical methods like Finite Difference Method (FDM) and Finite Element Method (FEM) can be used. FEM provides approximate values at discrete points in the domain. It breaks down a large problem into smaller finite elements. These element's equations are combined into a system representing the whole problem. We show the comparison between analytic solution, solutions by FDM and FEM. The impact of heat on the material is examined at various positions and multiple positions. We compare the analytical and numerical (by FEM) solution considering several homogeneous materials with various diffusivity values (α). Finally, the simulation results of different non-homogeneous materials were compared. Science and engineering fields that use heat equations can be evaluated using the numerical method applied here.

Submitted: July 3, 2024; **Revised**: May 30, 2025; **Accepted**: June 1, 2025

Keywords: Analytical solution; Finite element method; Heat equation; Numerical solution; Partial differential equation.

I. INTRODUCTION

The heat equation, commonly referred to as the diffusion equation, is a partial differential equation (PDE) utilized to characterize the progression of heat distribution in a solid medium over time [2, 4]. It illustrates how temperature (or heat distribution) changes over time in a specific area. The applications of the heat equation include particle diffusion, Brown's law of motion, the equation of Schrodinger for an unbound particle and the thermal dispersion in polymers [2]. Additionally, it is utilized in picture evaluation, the spatial environmental model, the cancer model, and the exterior layer of rockets, trains, bridges and the freezers. As a result, many different scientific domains place a high value on the heat equation [2, 4, 5, 7].

A fundamental concept of thermodynamic is heat transfer, where heat transfers from a region of higher temperature to the lower temperature resulting the change in temperature of both regions [10]. Assuming that the system does not perform any work and there is no change of phase, the temperature of colder body rises while the temperature of hotter body drops. The extent of heat transfer is influenced by three primary parameters: change of the temperature, substance phase and mass of the system [10]. In real-world applications like metal working, accurate heat regulation is essential. Varying amount of heat may be used in different parts of materials to give them the right shape without producing unwanted phase shift or structural damage. For instance, in forging or welding, requires precise temperatures for metals to become malleable or to form a correct bond. This application of heat ensures the metal may be manipulated into desired form that shows the role of controlled heat in industrial process [10]. So, understanding the relation among heat, temperature change and characteristics of materials is important for enhancing these processes and achieving high quality results. Let $u = u(x,t)$, then the PDE of the form [2]

$$\begin{aligned} u_t(x,t) &= \alpha u_{xx}(x,t),\ \alpha > 0 \\ \text{BCs} &: u(0,t) = T_1, u(L,t) = T_2;\ t > 0 \\ \text{IC} &: u(x,0) = f(x);\quad 0 \le x \le L \end{aligned} \tag{1}$$

where T_1, T_2 represent boundary temperatures, $f(x)$ denotes the initial heat amount at position x along the rod and α is referred as thermal diffusivity, is referred to as a one-dimensional diffusion or heat equation [2]. It serves

*)Corresponding author: jeevan.kafle@cdmath.tu.edu.np

(a) (b)

Figure 1: Heating of different materials (a) Iron rod (b) Glass [18].

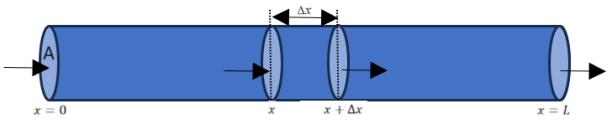

Figure 2: Heat flow in a rod.

as an illustration of a typical partial differential equation that is parabolic. When the domain has a regular geometry, there is an analytical solution of the heat equation; however, when the domain has an irregular form, computation of the analytical solution of those equations is particularly challenging [11, 16]. As a result, estimation of the solution of the modeled PDEs is done using numerical techniques. Here, we focus on Finite Difference Method (FDM) and Finite Element Method (FEM). The finite difference method is considered as one of the numerical techniques utilized to determine solutions for PDEs through the procedure of breaking up the domain into a finite number of distinct components. These solutions are then computed at the domain's particular grid points [12, 17].

The process of finite element method involves the discretization of domain to obtain simplified equations of finite element, assemble these equations, apply initial conditions with boundary constraints, solve the problem and provides postprocessing (visualization) [16, 18]. When a domain (a geometric region) is meshed, it is decomposed into a series of discrete (here finite) elements. The mesh elements must closely follow and accurately represent the geometry to provide a good approximation. The nodes serve as link between adjacent elements [16, 18]. Simply, node is a point in an area that is identified by its coordinates. A discretization strategy divides a continuum into finite sub-divisions connected at nodes and is referred to a well defined set of procedure that include: (i) the generation of meshes with finite elements (ii) how basis functions are defined for reference elements (also known as shape functions), and (iii) the process of translating reference elements onto mesh elements. Finite element method is based on several other, more-fundamental, approximate techniques like: (i) Rayleigh-Ritz method, ii) Galerkin Method, iii) Petrov-Galerkin method, and iii) Least square method [16, 18]. The utilization of FEM proves to be highly beneficial in the creation of stiffness and strength visualizations as well as in the reduction of weights, materials, and costs. It enables a comprehensive visualization at structural bending or twisting, and indicating the displacements as well as stresses distribution [18].

The formulation of the heat equation is attributed to Jean-Baptise Joseph Fourier (1768-1830), who initially submitted this as a draft in 1807 AD, to the institute de France and published in 1822 AD as his work Analytic Theory of Heat [12]. In context of production or consumption of internal heat, Chamkha and Khaled [3] state that the impact of magnetized field on simultaneous transfer of mass and heat through a stagnant flow that is linearly stratified experiences mixed convection. The finite difference method (FDM) was first presented in 1715 by Brook Taylor. Since then, the concept of FDM has been studied as an conceptual, autonomous mathematical idea by George Boole (1860), C.M. Thomson (1933), and Karaly Jordan (1939) [11, 16]. Makhtoumi [8] conducted a study on solving the heat diffusion analytically and numerically within a thin rod on one dimension, utilizing the PDE system of rod for the application of the Finite Difference Method (FDM). A simple heat equation problem in one dimension was studied by Olaiju et al. [13, 14] using the explicit finite difference scheme. Kafle et al. [9] applied forward time central space scheme to develop a numerical solution for the heat equation in one dimension and Kandel et al. [10] used them in the impact of the source on the heat transformation through numerical modelling.

Finite element method's origins can be traced to the early 1940s, when academics started creating numerical methods for resolving challenging engineering issues [16]. One of the first developers of the finite element approach was Richard Courant [18]. His focus was on applying this method to address partial differential equations, particularly in solid mechanics and structural analysis. Originally, the word finite element was used in 1960 by Clough [18]. Since then, the technique has been expanded to include the numerical modeling of physical structures in many other engineering fields, like fluid dynamics, heat transport, and electromagnetism [16]. Dabral et al. [4] studied the B-Spline Finite Element Method to numerically simulate the Heat Equation in one dimension while considering the B-spline basis function.

The majority of current research focuses on homogeneous materials or regular domains, despite the fact that both the Finite Element Method (FEM) and the Finite Difference Method (FDM) are frequently utilized to solve heat transfer problems. With regard to non-homogeneous ma-

terials, where spatial changes in thermal characteristics have a substantial impact on the solution, this work offers a comparative numerical study. The novelty lies in the direct evaluation of FEM, including accuracy, stability, and its ability to capture gradients in complex material distributions. Our work primarily focuses on using FDM and FEM to numerically solve parabolic partial differential equation in one dimension. The formulation of numerical methods is addressed in the second section. The third section illustrates the comparison between analytic solution, solutions by FDM and FEM along with the error analysis. This section also includes the impact of applying heat to the substance at different and multiple positions, as well as a comparison of solutions made of materials with varying diffusivity along with the simulation results of different non-homogeneous materials. The work's conclusion and findings are summarized in the fourth section.

II. NUMERICAL METHODS

FEM is based on approximate techniques like Rayleigh-Ritz method, Galerkin Method, Petrov-Galerkin method and Least square method [6, 16]. Here we use **Galerkin Method**. The fundamental principle of the Galerkin technique is to project the solution of a PDE onto a finite-dimensional subspace, which is often bounded by a collection of basis functions. Over the relevant domain, these basic functions constitute an entire and linearly independent set. The Galerkin technique looks for a roughly correct answer that minimizes the PDEs' residual error [4].
Let $u \in \mathbf{H}_0^1([0,L])$ where,

$$\mathbf{H}_0^1([0,L]) = \left\{ v : \int_0^L v^2 dx < \infty, \int_0^L v_x^2 dx < \infty; \right\}$$

$$\{v(0) = v(L) = 0\} \tag{2}$$

Also, let V_d be subspace of $\mathbf{H}_0^1([0,L])$ and $\dim(V_d) = n+1$. Suppose $u_d \in V_d$ is approximation solution of (1) i.e., $u \approx u_d$. Substituting $u = u_d$ in (1),

$$(u_d)_t - \alpha(u_d)_{xx} = R(x) \neq 0 \tag{3}$$

where R(x) is known as residual error [4, 11]. By Galerkin method [4, 11],

$$\int_0^L R(x) v_d dx = 0, \forall v_d \in V_d \tag{4}$$

$$or, \int_0^L (u_d)_t v_d dx = \alpha \int_0^L (u_d)_{xx} v_d dx \tag{5}$$

The weak formulation of (5)

$$\begin{aligned}\int_0^L \frac{\partial u_d}{\partial t} v_d dx &= \alpha \left[v_d \int_0^L (u_d)_{xx} dx - \int_0^L \frac{\partial v_d}{\partial x} \int_0^L (u_d)_{xx} dx \right] \\ &= \alpha \left[v_d \frac{\partial (u_d)_x}{\partial x} \right]_0^L - \alpha \left[\int_0^L \frac{\partial v_d}{\partial x} \frac{\partial u_d}{\partial x} \right] dx \\ &= -\alpha \int_0^L \frac{\partial v_d}{\partial x} \frac{\partial u_d}{\partial x} dx\end{aligned}$$

$$\text{Thus, } \int_0^L \frac{\partial u_d}{\partial t} v_d dx = -\alpha \int_0^L \frac{\partial v_d}{\partial x} \frac{\partial u_d}{\partial x} dx \tag{6}$$

Linear basis functions of V_d are chosen on $[x_i, x_{i+1}]$, $i = 1, 2, \cdots, n$. The basis function $\phi_i(x)$ $(i = 1, 2, 3, \cdots, n+1)$ is defined by [4, 11]

$$\phi_1(x) = \begin{cases} \frac{x_2 - x}{h} & \text{for } x_1 \leq x \leq x_2, \\ 0 & \text{otherwise} \end{cases} \tag{7}$$

$$\phi_{n+1}(x) = \begin{cases} \frac{x - x_n}{h} & \text{for } x_n \leq x \leq x_{n+1}, \\ 0 & \text{otherwise} \end{cases} \tag{8}$$

For $i = 2, 3, \cdots, n$,

$$\phi_i(x) = \begin{cases} \frac{x - x_{i-1}}{h} & \text{for } x_{i-1} \leq x \leq x_i, \\ \frac{x_{i+1} - x}{h} & \text{for } x_i \leq x \leq x_{i+1}, \\ 0 & \text{otherwise} \end{cases} \tag{9}$$

The linear basis functions $\phi_i(x)$ have a value of 1 at their respective nodes and 0 at other nodes [4].

$$u_d(x,t) = \sum_{i=1}^{n+1} u_i(t)\phi_i(x) \text{ and } v_d(x,t) = \sum_{j=1}^{n+1} v_j(t)\phi_j(x) \tag{10}$$

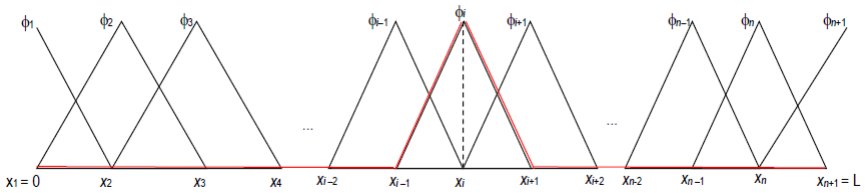

Figure 3: Discretized domain and bases functions [11].

Using (6) and (10), the weak formulation becomes [11]

$$\int_0^L \frac{\partial}{\partial t}\left[\sum_{i=1}^{n+1} u_i(t)\phi_i(x)\right]\sum_{j=1}^{n+1} v_j(t)\phi_j(x)dx = -\alpha\int_0^L \frac{\partial}{\partial x}\left[\sum_{i=1}^{n+1} u_i(t)\phi_i(x)\right] \frac{\partial}{\partial x}\left[\sum_{j=1}^{n+1} v_j(t)\phi_j(x)\right]dx$$

$$\text{or, } \int_0^L \left[\sum_{i=1}^{n+1} \dot{u}_i(t)\phi_i(x)\phi_j(x)\right]dx = -\alpha\int_0^L \left[\sum_{i=1}^{n+1} u_i(t)\frac{d\phi_i(x)}{dx}\frac{d\phi_j(x)}{dx}dx\right]$$

$$\text{or, } \sum_{i=1}^{n+1} \dot{u}_i(t)M_{ij} = -\alpha\sum_{i=1}^{n+1} u_i(t)A_{ij}$$

$$\text{or, } \dot{u}_1(t)M_{1j} + \dot{u}_2(t)M_{2j} + \ldots + \dot{u}_{n+1}(t)M_{n+1j} = -\alpha\left[u_1(t)A_{1j} + u_2(t)A_{2j} + \cdots + u_{n+1}(t)A_{n+1j}\right]$$

This can be written as

$$\dot{u}(t)M + \alpha A u(t) = 0 \tag{11}$$

where

$$(t) = [u_1(t)\ u_2(t)\cdots u_{n+1}(t)]^T \text{ and } \quad \dot{u}(t) = \frac{du}{dt}$$

$$M_{ij} = \int_0^L \phi_i(x)\phi_j(x)dx, \quad A_{ij} = \int_0^L \frac{d\phi_i(x)}{dx}\frac{d\phi_j(x)}{dx}dx$$

By using Forward Difference Method in (11) [9], we get,

$$u_m^{n+1} = Cu_m^n, \text{ where } C = I - \alpha\Delta t M^{-1}A \tag{12}$$

III. RESULTS AND DISCUSSION

A. Comparison Between Analytical, FDM and FEM

We take the following example of heat equation: [9]

$$u_t = 0.05u_{xx}; \quad 0 \le x \le 1, \quad t \ge 0 \tag{13}$$
$$\text{BCs} : u(0,t) = u(L,t) = 0; \quad t > 0$$
$$\text{IC} : u(x,0) = \sin\pi x; \quad 0 \le x \le 1$$

1. Analytical Solution

Applying Boundary and initial conditions, the analytic solution of (13) is [9],

$$u(x,t) = \sin(\pi x)\, e^{-0.05\pi^2 t} \tag{14}$$

Now, we are currently focused on determining the temperature distribution of a rod at distance $x = 0.8\,\text{m}$ from its initial point at a time $t = 0.8\,\text{hr}$. Using (14), we get, $u(0.8, 0.8) = 0.3961$

2. Numerical Solution by FDM

For the heat equation (13) above, the FTCS scheme is [9]

$$v_m^{n+1} = v_m^n + c\,(v_{m+1}^n - 2v_m^n + v_{m-1}^n)$$

with $v_0^n = v_M^n = 0$, $v_m^0 = \sin(\pi m h)$ and $c = \dfrac{0.005k}{h^2}$. The length of time and space intervals are $k = 0.2$ and $h = 0.2$ respectively [9]. According to Kafle et al. [9], numerical solution of equation (13) at distance $x = 0.8\,\text{m}$ from its initial point at a time $t = 0.8\,\text{hr}$ is

$$u_{\text{approx}} = v_4^4 = 0.3934$$

3. Numerical Solution by FEM

Applying the above equation (12) for the heat equation (13) we get,

$$u_m^{n+1} = Cu_m^n, \text{ where } C = I - 0.05\Delta t M^{-1} A \tag{15}$$

Let the space intervals and time length be $h = 0.2$ and $\Delta t = k = 0.2$ respectively. Now, solving it, we have

$v_0^0 = 0$	$v_1^0 = 0.5878$	$v_2^0 = 0.9511$	$v_3^0 = 0.9511$	$v_4^0 = 0.5878$	$v_5^0 = 0$
$v_0^1 = 0$	$v_1^1 = 0.5319$	$v_2^1 = 0.8604$	$v_3^1 = 0.8604$	$v_4^1 = 0.5319$	$v_5^1 = 0$
$v_0^2 = 0$	$v_1^2 = 0.4814$	$v_2^2 = 0.7783$	$v_3^2 = 0.7783$	$v_4^2 = 0.4814$	$v_5^2 = 0$
$v_0^3 = 0$	$v_1^3 = 0.4356$	$v_2^3 = 0.7041$	$v_3^3 = 0.7041$	$v_4^3 = 0.4356$	$v_5^3 = 0$
$v_0^4 = 0$	$v_1^4 = 0.3942$	$v_2^4 = 0.6369$	$v_3^4 = 0.6369$	$v_4^4 = 0.3942$	$v_5^4 = 0$
$v_0^5 = 0$	$v_1^5 = 0.3568$	$v_2^5 = 0.5761$	$v_3^5 = 0.5761$	$v_4^5 = 0.3568$	$v_5^5 = 0$

4. Comparison

The 3D-plots obtained from computational software of analytical and numerical solutions of equation (13) is shown in the Figure 4. These graphs visualize the solution of the temperature distribution u as a function of time t and space x through 3D surface plots. The color gradients indicate the magnitude of u, while color bars act as a point of reference for these values. The axes show u on the vertical axis while t and x on the horizontal planes. The shapes, contours, and color distributions of the analytic and numerical solutions exhibit similarities, implying that the numerical methods effectively approximate the analytic solution. The close visual similarities, especially in the color patterns, peaks, and valleys, indicates that the numerical solutions capture the main behavior of the system described by the analytic solution.

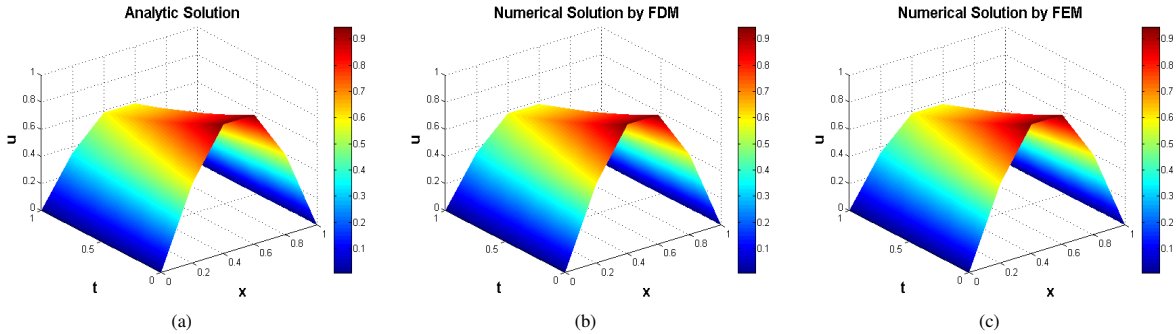

Figure 4: Analytical and Numerical solutions of one-dimensional Heat equation (13).

5. Error Analysis

Finally, in this analysis, the error is calculated at $x = 0.8$ m and $t = 0.2, 0.4, 0.6, 0.8$ and 1 hr. This is shown in a Table I. Here, E_D, E_E, $\%E_D$, and $\%E_E$ represent error by FDM, error by FEM, error percentage by FDM and error percentage by FEM respectively.

TABLE I: Comparison of analytical and numerical solutions for error analysis.

Values	Solutions by			E_D	E_E	$\%E_D$	$\%E_E$
	Analytical	FDM	FEM				
v_4^1	0.5325	0.5317	0.5319	0.0008	0.0006	0.15%	0.11%
v_4^2	0.4825	0.4809	0.4814	0.0016	0.0011	0.33%	0.23%
v_4^3	0.4371	0.4350	0.4356	0.0021	0.0015	0.48%	0.34%
v_4^4	0.3961	0.3934	0.3942	0.0027	0.0019	0.68%	0.48%
v_4^5	0.3588	0.3559	0.3568	0.0029	0.0020	0.80%	0.56%

Therefore, based on the information presented in the above Table I, it can be concluded that the numerical solutions provided by Finite Element Method (FEM) shows a higher level of accuracy compared to those obtained through Finite Difference Method (FDM). The reason for the improved accuracy of FEM's approximation of the solution might be related to its flexibility in managing complex geometries and boundary conditions. Consequently, it is evident that FEMs represent a more superior approach in comparison to FDMs when it comes to the computation of solutions for the one-dimensional heat equation.

As FEM is derived from a weak formulation of the heat equation, its objective is global error minimization across the entire domain, rather than an approximation of the differential equation at finite points (as in FDM). This makes the method more stable and convergent, particularly in cases with complex boundaries. Further, FEM uses unstructured mesh such as triangles and quadrilaterals, which are more tolerant of irregular geometries and non-uniform boundaries. Thus, FEM can more accurately predict local variations in the temperature field due to its spatial flexibility.

B. Variation of Initial Condition

Now, let's look at an illustration of the heat equation in one dimension for an iron rod, characterized by its thermal diffusivity 0.23 $cm^2s^{-1} = 0.000023$ m^2s^{-1} at 26.85°C temperature [10] given as:

$$u_t = 0.000023u_{xx} \quad 0 \le x \le 1, \quad t \ge 0 \tag{16}$$

$$\text{BCs} : u(0,t) = u(1,t) = 0; \quad t > 0$$

Now, we apply three different initial conditions for different experiments with the space intervals and time length $h = 0.1$ and $k = 0.2$ respectively while using FEM.

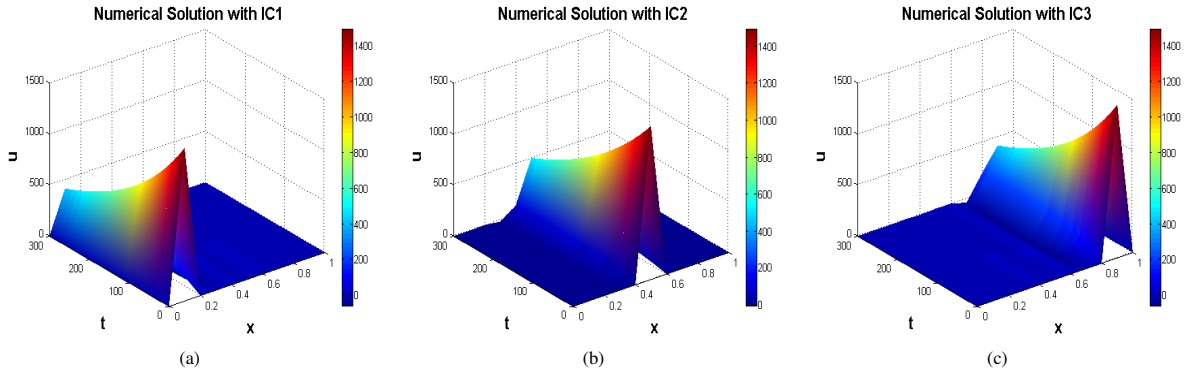

Figure 5: Temperature distribution corresponding to (a): IC1, (b): IC2, (c): IC3.

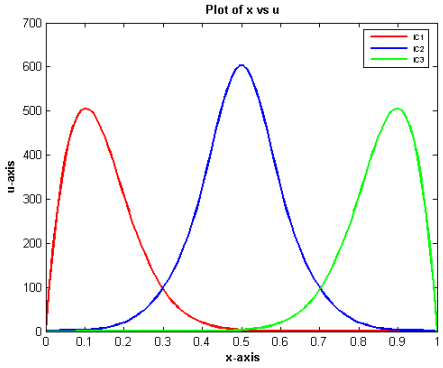

Figure 6: Plot of x against u following the application of 250 sec. of heat.

1. Variation of Position of Initial Condition

Initially, the discussion is about the variation in position of the initial condition, specifically focusing on the rod's left, middle, and right end within the context of the heat equation (16) provided above by using FEM. In this scenario, the initial conditions involve applying temperature of 1500°C in the rod close to the left, at the middle, and close to the right end having a length of 1m successively, given as:

$$\begin{aligned}&\text{IC1: } u(0.1,0) = 1500;\\ &\text{IC2: } u(0.5,0) = 1500;\\ &\text{IC3: } u(0.9,0) = 1500.\end{aligned}$$

$$v_m^0 = \begin{cases} 1500 & \text{for } m = 3,7 \\ 0 & \text{otherwise} \end{cases} \qquad \text{and} \qquad v_m^0 = \begin{cases} 1500 & \text{for } m = 2,5,8 \\ 0 & \text{otherwise} \end{cases}$$

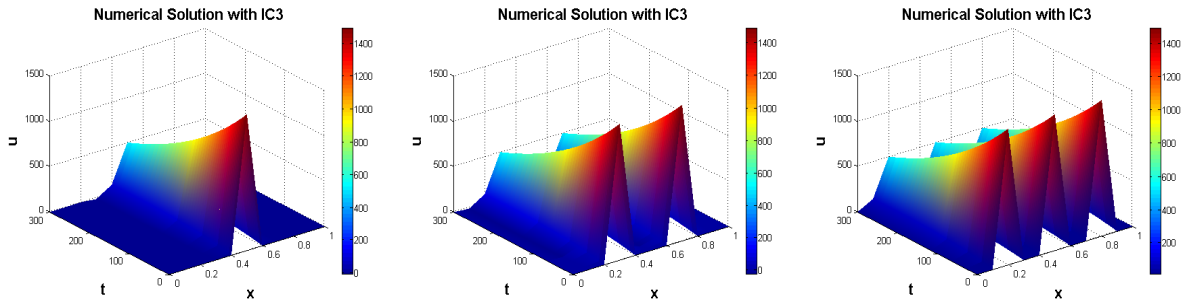

Figure 7: Temperature distribution corresponding to (a): IC1, (b): IC2, (c): IC3.

The temperature distribution up to 300 sec. after the material is heated is shown in Figure 7 with various initial conditions, namely IC1, IC2, and IC3. Figure 7 shows that the material's temperature, i.e., of the iron rod, steadily drops off after heating. The rod gradually cooled from 1500°C to about 500°C in approximately 300 sec.

With the help of FEM the nature of heat distribution is then studied in the rod. The following Figure 5 displays the temperature distributions for the three cases mentioned above. We can see from Figure 5 that heat can only move in one direction, i.e., to the right and left, respectively with IC1 and IC3. However, heat can follow in both way with IC2. Additionally, a plot of x against u (distribution of temperature) is given by Figure 6. The iron rod in the first and third cases is only around 500°C, after heating for 250 sec. but Figure 6 demonstrates the rod is approximately around 600°C in the second case. At both ends, the boundary conditions set to 0°C, are the reason of this variation. Applying heat to the near left and near right yields identical results. Nevertheless, if the substance wasn't homogeneous or if the left and right ends' boundary conditions were different, the result would be more fascinating.

2. Initial Condition in Multiple Position

This is a generalization of the above idea considering various initial conditions. Considering initial condition (IC1) that comes first, we have

$$v_m^0 = \begin{cases} 1500 & \text{for } m = 5 \\ 0 & \text{otherwise} \end{cases}$$

In the same way, considering IC2 and IC3, respectively the initial conditions, we get

As previously mentioned, we heated the rod at one place in IC1, at two and three places in IC2 and IC3, respectively. In Figure 7, the numerical solution has a redder and browner frontal border with IC3. It indicates, in comparison to ICs 1 and 2, the temperature distribution of the rod is more uniform in IC3. This is due to an increase

in the number of locations that provide heat. Blacksmiths and goldsmiths were among the metal workers who employed this technique for heating items such as iron rods.

Figure 8 shows that after 250 seconds of applying heat to the iron rod, the average temperature is about 590°C. The figure illustrates that, due to supply of heat in additional locations than IC1 and IC2, IC3's average rod's temperature is higher than IC2's and IC1's. Consequently, we draw conclusion that the number of heat applied locations is proportionate to the iron rod's average temperature.

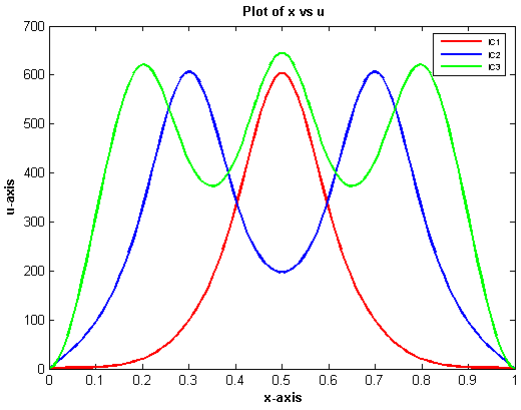

Figure 8: Plot of x against u following the application of 250 sec. of heat.

C. Variation of Diffusivity of Materials

1. Homogeneous Materials

The heat equation's analytical and numerical (by FEM) solutions for rods made of three distinct homogeneous materials namely Nylon ($\alpha = 0.09$ mm^{2}s^{-1}), Glass ($\alpha = 0.34$ mm^{2}s^{-1}) and Quartz ($\alpha = 1.4$ mm^{2}s^{-1}) [9] are compared in this section.

TABLE II: Comparison of analytic and numerical solution at $x = 0.8$ mm and $t = 2$ sec.

Materials	Diffusivity (mm^{2}s^{-1})	Analytic Solution [9]	Numerical Solution (by FEM)	Error	% Error
1. Nylon	0.09	0.0995	0.0997	0.002	0.20%
2. Glass	0.34	7.1536×10^{-4}	7.1873×10^{-4}	3.37×10^{-6}	0.47%
3. Quartz	1.4	5.8551×10^{-13}	5.5432×10^{-13}	3.12×10^{-14}	5.33%

According to the Table II, the percentage errors for the substances Quartz, Glass, and Nylon are 5.33%, 0.47%, and 0.20%, respectively. Thus, we also determine that, in comparison to the exact solution, materials with higher diffusivity have more numerical error. Therefore, when dealing with substances that have lesser diffusivity, numerical solutions (by FEM) are far more appropriate. In comparison to materials with greater diffusivity, we find that FEM provides a superior approximation for materials with lesser diffusivity values.

It is evident from the top panels (Figure 9I) that heat spreads more slowly on the rod than it does in the middle panel (Figure 9II), and the bottom panel (Figure 9III) shows a significantly shorter period. We thus draw the conclusion that materials with lower diffusivity will take longer to cool down than materials with greater diffusivity because lower diffusivity results in slower heat dispersion in the rod. Because of this, heat is transferred and lost instantly for higher diffusivity materials.

Additionally, we noticed the materials temperature is rising more quickly in the bottom panels of (Figure 9III) than in the middle panels of (Figure 9II) and faster in the middle panels of (Figure 9II) than in the top panels of (Figure 9I). Thus, we argue that the temperature of a material with a greater diffusivity rises more quickly than that of a substance with a lower diffusivity. As a result, the distribution of temperature of the rod $u(x,t)$ and the material's diffusivity (α) are directly proportional.

We conclude that, how quickly heat moves through a substance is determined by its thermal diffusivity. The temperature gradients throughout the domain are smoother when the diffusivity is higher because it causes faster and more even heat transfer. On the other hand, lower diffusivity slows down the heat transmission process, which results in sharper gradients and a more localized temperature. The temperature profile's structure and evolution over time are directly influenced by this behavior, with higher diffusivity encouraging quicker thermal equilibrium.

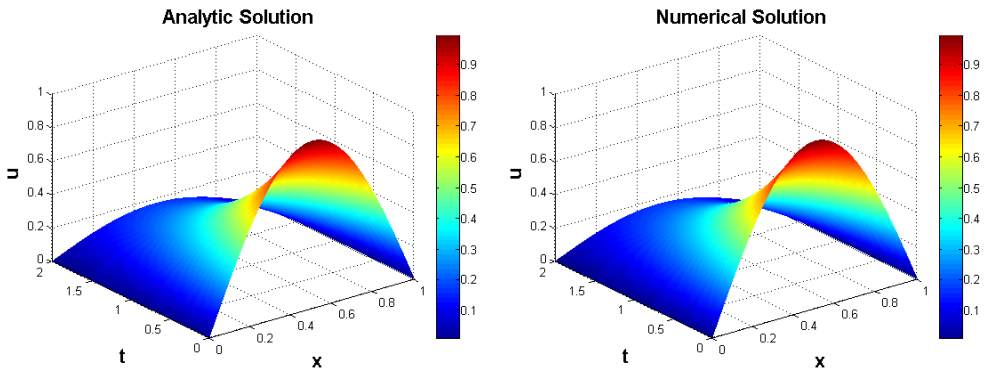

(I) Nylon ($\alpha = 0.09$ mm^{2}s^{-1})

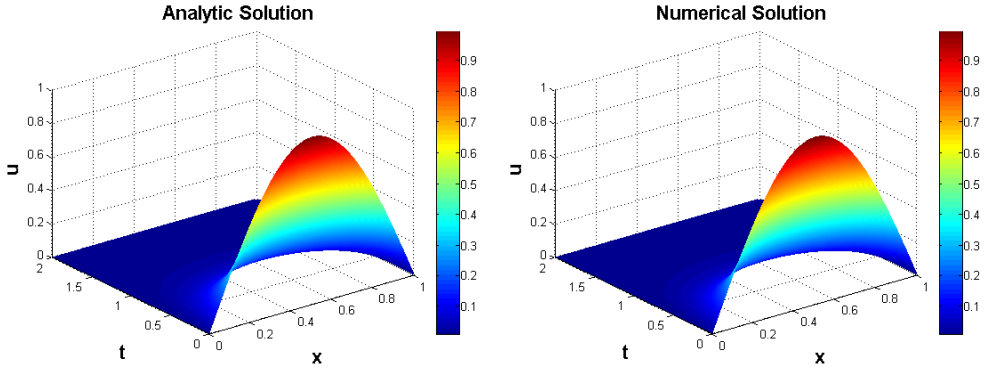

(II) Glass ($\alpha = 0.34$ mm^{2}s^{-1})

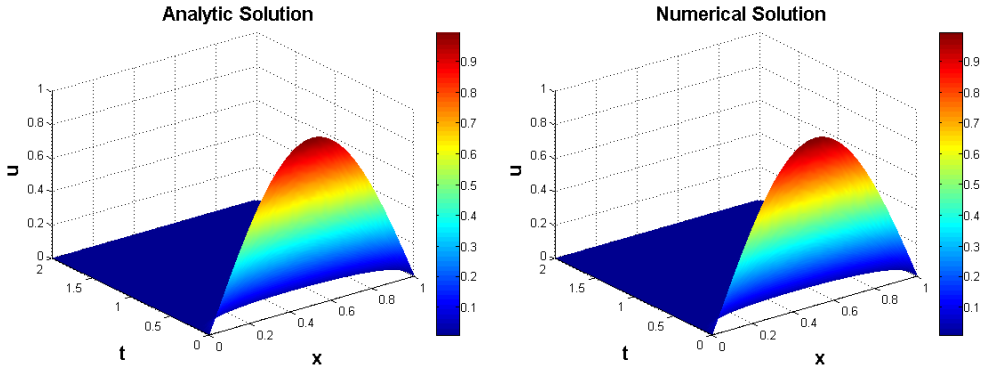

(III) Quartz ($\alpha = 1.4$ mm^{2}s^{-1})

Figure 9: Analytic and numerical solution of heat equation 1 (with $m = 50$ and $n = 1000$) having $T_1 = T_2 = 0$, $f(x) = T_0 = \sin\pi x$ for different values of α.

2. *Non-Homogeneous Materials*

The materials found in nature are often non-homogeneous. In this section, we analyze heat transfer in one dimensional rod made up of two distinct substances. Next, we examine the simulation's findings for heat flow from materials with low diffusivity to those with high diffusivity and vice versa applying FEM, where a rod's total length is maintained constant ($L = 1$ m) with a homogeneous

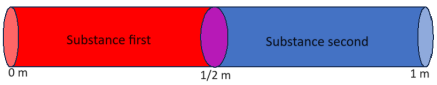

Figure 10: Rod (non-homogeneous) made up of two distinct substances.

radius and is made up of two materials with the same length, meaning that every substance has a length 0.5 m. For this problem, the appropriate PDE is

$$u_t = \begin{cases} \alpha_1 u_{xx} & \text{for} \quad 0 \le x \le 0.5 \\ \alpha_2 u_{xx} & \text{for} \quad 0.5 \le x \le 1 \end{cases} \tag{17}$$

where diffusivity of substances first and second is represented by α_1 and α_2, respectively. Also,

BCs: $u(0,t) = u(1,t) = 0; \quad t > 0$
IC: $\quad u(x,0) = \sin \pi x; \quad 0 \le x \le 1$

Initially, we assume that substance first is Nylon and substance second is Quartz. Next, we take substance first Quartz and substance second Nylon into consideration. Both Nylon and Quartz have diffusivity values of 0.09 mm^2s^{-1} and 1.4 mm^2s^{-1} respectively. We take Nylon ($\alpha = 0.09$ mm^2s^{-1}) as substance first and Quartz ($\alpha = 1.4\, mm^2s^{-1}$) [9] as substance second in Figure 11(a) . Heat therefore moves from a substance with low diffusivity to one with high diffusivity. In this instance, the left portion of the material (substance first) has low diffusivity, which causes heat to move forward slowly and raise the temperature. On the other hand, the right part of the material (substance second) has high diffusivity, which causes heat to flow faster and raise the temperature quickly. However, we modified substance first to be Quartz ($\alpha = 1.4$ mm^2s^{-1}) and substance second to be Nylon ($\alpha = 0.09$ mm^2s^{-1}) [9] in Figure 11(b). Heat transfers from a substance with a high diffusivity to one with a low diffusivity in this instance.

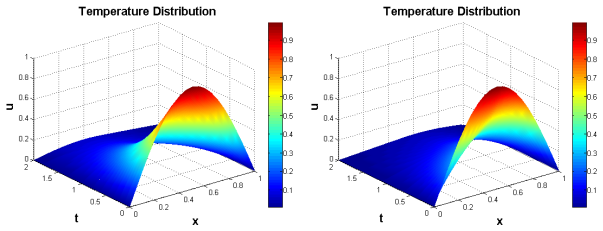

Figure 11: Distribution of temperature with (a) Quartz at right and Nylon at left (b) Nylon at right and Quartz at left.

Figure 12 depicts the temperature distribution (u) plotted against various time levels $t = 0.5$ s, 1 s, 1.5 s, and 2 s, showcasing Nylon on the left and Quartz on the right in scenario (a), and Quartz on the left with Nylon on the right in scenario (b). The maximum temperature distribution (u) at each time are around $x = 0.4$ m and $x = 0.65$ m shown in Figure 12(a) and Figure 12(b), respectively. This is a result of heat flowing more slowly in the left half of Figure 12(a) (low diffusivity material) and more swiftly in the left half of Figure 12(b) (high diffusivity material). Because of the gradual distribution of temperature in the left half section of Figure 12(a) (low diffusivity material in left half), the maximum value of u in Figure 12(a) [0.485] over time $t = 2$ s is larger than in Figure 12(b) [0.435]. We get the conclusion that heat moves more quickly through the portion made of higher diffusivity material and more slowly through the section made of lower diffusivity material. It is possible to use and expand this computational method to non-homogeneous materials that are present in nature.

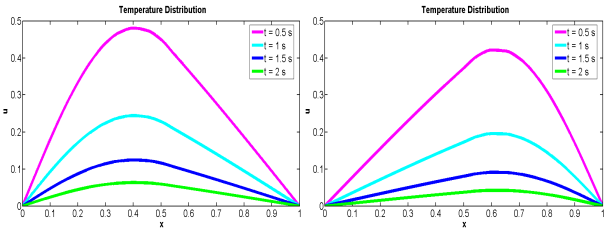

Figure 12: Plot of x versus u at multiple time levels $t = 0.5$ s, 1 s, 1.5 s, and 2 s with (a) Quartz at right and Nylon at left (b) Nylon at right and Quartz at left.

IV. CONCLUSION

The work concludes that one dimensional parabolic partial differential equations can be numerically solved with the help of the Finite Difference Method (FDM) and Finite Element Method (FEM). When analytical solutions are not feasible because of complicated boundary conditions or irregular domains, these techniques offer effective solutions. The study shows the accuracy and dependability of numerical methods in approximating solutions by comparing the analytic solution with solutions derived by FDM and FEM and concludes that FEMs are better methods then FDMs to compute the solutions of one dimensional heat equation. We examined a one dimensional heat equation with various initial condition locations on a rod by using FEM. Temperature of 1500°C is applied at different positions on the rod. Heat distribution within the rod is investigated. Temperature lasts longer at the center due to selected boundary conditions. Iron rod heated at one, two, and three positions; more locations lead to

higher average temperature. Study on heat transfer with different diffusivity (α) shows quicker temperature rise with higher diffusivity. Higher diffusivity materials experience instantaneous heat loss and transmission. Finite Element Method is preferred for lower diffusivity materials due to fewer errors. Non-homogeneous materials show quicker temperature increase in higher diffusivity parts, while slower in lower diffusivity parts of the rod. Natural non-homogeneous materials can be addressed using our computational method. The Finite Element Method (FEM) has limits even though it has shown exceptional accuracy and adaptability while working with complex geometry. Notably, FEM can be computationally costly, particularly when dealing with time-dependent problems or tiny meshes. Its capacity to scale to higher dimensions like complete 2D and 3D heat transfer simulations, requires a large amount of processing power and precise mesh creation.

In the future, research might be done on anisotropic materials or nonlinear boundary conditions to expand the current methodology to investigate instantaneous heat conduction in 2D and 3D domains. These additions would improve FEMs applicability for practical engineering issues such as electronic devices, biological simulations, and thermal analysis of multi-layer composites.

REFERENCES

1. A. Z. Azmi, *Numerical Solution for Heat Equation*. Thesis of Bachelor of Science (Industrial Mathematics), Faculty of Science, University Teknologi Malaysia, 2009.
2. W. E. Boyce, R. C. DiPrima and D. B. Meade, *Elementary Differential Equations and Boundary Value Problems*, Loose-Leaf Print Companion. John Wiley and Sons, 2017.
3. A.J. Chamkha and A.A. Khaled, Hydromagnetic combined heat and mass transfer by natural convection from a permeable surface embedded in a fluid-saturated porous medium, *International Journal of Numerical Methods for Heat and Fluid Flow*, **12**(8), 234-250, 2000.
4. V. Dabral, S. Kapoor and S. Dhawan, Numerical Simulation of one dimensional Heat Equation: B-Spline Finite Element Method. *Indian Journal of Computer Science and Engineering* (IJCSE), 2(2), 222-235, 2011.
5. M. Dehghan and S. Kazem, Application of finite difference method of lines on the heat equation. *Wiley Periodicals, Inc* (Doi: 10.1002/num.22218), 2017.
6. B. D. Hahn and D.T. Valentine, Essential MATLAB for Engineers and Scientists, Third edition, Elsevier, 428 p, 2007.
7. T. Hayat, A.H. Kara and E. Momoniat, The unsteady flow of a fourth-grade fluid past a porous plate. *Journal Applied mathematics and computation*, **200**, 65-76, 2005.
8. M. Makhtoumi, Numerical Solutions of Heat Diffusion Equation Over One Dimensional Rod Region. *International Journal of Science and Advanced Technology*, **7**(3), 10-13 (ISSN:2221-8386), 2017.
9. J. Kafle, L. P. Bagale and D. K. C., Numerical Solution of Parabolic Partial Differential Equation by Using Finite Difference Method. *J. Nep. Phys. Soc.*,**6**(2): 57-65, 2020.
10. H. P. Kandel, J. Kafle and L. P. Bagale, Numerical Modelling on the Influence of Source in the Heat Transformation: An Application in the Metal Heating for Blacksmithing. *J. Nep. Phys. Soc.*,**7**(2): 97-101, 2021.
11. B. Mebrate, Numerical Solution of a One Dimensional Heat Equation with Dirichlet Boundary Conditions. *American Journal of Applied Mathematics*, **3**(6), 305-311 (doi: 10.11648/j.ajam.20150306.20), 2015.
12. T.N. Narasimhan, *Fourier's Heat Conduction Equation: History,Influence, and Connections*, Lawrence Berkeley National Laboratory University of California, Berkeley, 1999.
13. O. A. Olaiju, Y.S. Hoe and E. B. Ogunbode, Finite-Difference Approximations to the Heat Equation via C. *Journal of Applied Sciences & Environmental Sustainability*, **3**(7), 188-200, 2017.
14. O. A. Olaiju, Y.S. Hoe, and E. B. Ogunbode, Finite Element and Finite Difference Numerical Simulation Comparison for Air Pollution Emission Control to Attain Cleaner Environment. *Chemical Engineering Transactions*, **63**, 679-684, 2018.
15. G.W. Recktenwald, *Finite Difference Approximations to the Heat Equation*,2011.
16. J. N. Reddy, *Solutions Manual for An Introduction to The Finite Element Method*, Forth Edition, McGraw-Hill, New York, 420 p,2006.
17. J.C. Strikwerda, *Finite Difference Schemes and Partial Differential Equations*, (2nd ed), 2004.
18. E. L. Wilson and R. E. Nickell, Application of the finite element method to heat conduction analysis. *Nuclear Engineering and Design*, **4**(3), 276-286 (doi.org/10.1016/0029- 5493(66)90051-3), 1966.